Structural Engineering and Mechanics, Vol. 30, No. 2 (2008) 247-261
DOI: http://dx.doi.org/10.12989/sem.2008.30.2.247

Finite element analysis of shear-deficient RC beams strengthened with CFRP strips/sheets

H. K. Lee†, S. K. Ha and M. Afzal

Department of Civil and Environmental Engineering, Korea Advanced Institute of Science and Technology, Guseong-dong, Yuseong-gu, Daejeon 305-701, Korea

(Received September 22, 2007, Accepted August 18, 2008)

Abstract. Performance of shear-deficient reinforced concrete (RC) beams strengthened with carbon fiber-reinforced polymer (CFRP) strips/sheets is analyzed through numerical simulations on four-point bending tests. The numerical simulations are carried out using the finite element (FE) program ABAQUS. A micromechanics-based constitutive model (Liang *et al.* 2006) is implemented into the FE program ABAQUS to model CFRP strips/sheets. The predicted results are compared with experiment data (Khalifa and Nanni 2002) to assess the accuracy of the proposed FE analysis approach. A series of numerical tests are conducted to investigate the influence of stirrup lay-ups on the shear strengthening performance of the CFRP strips/sheets, to illustrate the influence of the damage parameters on the microcrack density evolution in concrete, and to investigate the shear and flexural strengthening performance of CFRP strips/sheets. It has been shown that the proposed FE analysis approach is suitable for the performance prediction of RC beams strengthened with CFRP strips/sheets.

Keywords: finite element analysis; performance prediction; CFRP strips/sheets; micromechanics-based constitutive model; load-deflection curve.

1. Introduction

A majority of civil infrastructures presently used for various purposes call for retrofitting or strengthening primarily due to the substantial increment in service/live loads, severe environmental conditions, inappropriate construction, and insufficient maintenance (Lee *et al.* 2007). There are numerous articles reporting the behavior of plain beams reinforced externally with fiber-reinforced polymer (FRP) sheets or strips for the purpose of increasing the load-carrying capacity (see e.g., Jones *et al.* 1980, Saadatmanesh and Ehsani 1991, Chajes *et al.* 1994, Arduini *et al.* 1997, Norris *et al.* 1997, Oehlers *et al.* 2000, Jones *et al.* 2004, Jayaprakash *et al.* 2007). Shear strengthening of reinforced concrete (RC) beams using carbon FRP (CFRP) composites was systematically investigated by Khalifa *et al.* (2000). In their experimental study, two different FRP-based strengthening systems were investigated: externally bonded CFRP sheets and near surface mounted FRP rods. The test results confirmed that externally bonded CFRP sheets and CFRP rods could be used to increase significantly the shear performance.

Khalifa and Nanni (2002) examined the shear performance and modes of failure of rectangular

† Associate Professor, Corresponding author, E-mail: leeh@kaist.ac.kr

simply supported RC beams designed with shear deficiencies. The effect of external glass fiber-reinforced polymer (GFRP) plates on the flexural and shear behavior of structurally deficient RC beams was investigated by Leung (2002). It was shown from their experiment that the use of GFRP plates enhanced the strength and deformation capacity of RC beams by altering their failure modes. Wenwei and Guo (2006) carried out an experiment concerning flexural strengthening of RC beams by the externally bonding of CFRP laminates to the tension face of beams under different levels of sustaining loads. Niu *et al.* (2006) investigated materials configuration effect on strengthening of concrete slabs by CFRP composites. Most recently, Ghosh and Karbhari (2007) evaluated strengthening of FRP rehabilitated bridge decks after in-service loading.

While substantial experience with CFRP laminates retrofitting and its experimental verification exists in the infrastructure retrofitting and rehabilitation community, little knowledge exists on how the retrofitted infrastructure in service will perform. Accordingly, predictive analytical and numerical tools are required to evaluate the performance of the retrofitted infrastructure and to design CFRP laminates retrofitting. The present study is concerned with a finite element (FE) analysis approach for the evaluation of performance of shear-deficient RC beams strengthened with CFRP strips/sheets. Khalifa and Nanni (2002)'s experiments on RC beams strengthened with CFRP strips/sheets are chosen in the present study as a benchmark to numerically investigate the shear strengthening performance of CFRP strips/sheets. Using the FE program ABAQUS together with a micromechanics-based constitutive model for laminated composites (Liang *et al.* 2006) implemented into the FE program ABAQUS, a series of numerical four-point bending tests are conducted to evaluate the shear performance of RC beams strengthened with CFRP strips/sheets and to quantify shear strengthening performance of the CFRP retrofit systems. It should be noted that failure criteria are not considered in the present framework. The progressive loss of strength resulting from the nucleation of microcracks in concrete and debonding of fibers in the CFRP strips/sheets is incorporated into the constitutive model.

The numerical tests yield load-deflection curves from which shear strengthening performance of the CFRP strips/sheets is evaluated, and the predicted results are compared with experimental data (Khalifa and Nanni 2002) to assess the accuracy of the proposed FE analysis approach. A series of numerical tests are conducted to investigate the influence of stirrup lay-ups on the shear strengthening performance of the CFRP strips/sheets, to illustrate the influence of the damage parameters on the microcrack density evolution in concrete, and to investigate the shear and flexural strengthening performance of CFRP strips/sheets.

2. Constitutive model for CFRP strips/sheets

In our previous work published in Liang *et al.* (2006), a micromechanics-based constitutive model incorporating infinite cylindrical inclusions (Cheng and Batra 1999) was proposed to predict the overall elastic behavior of laminated composites. This section briefly summarizes the model derivation for the CFRP strips/sheets constitutive and damage modeling following the formulation of Liang *et al*. (2006).

Based on the governing field equations for linear elastic composites containing arbitrarily non-aligned and/or dissimilar inclusions (Ju and Chen 1994a, 1994b), in conjunction with the stiffness transformation law by Herakovich (1998), the stiffness matrix of off-axis unidirectional FRP sheets/strips $\overline{C}$ can be derived as (Liang *et al.* 2006)

$$\sigma = \overline{C}:\varepsilon \tag{1}$$

where the stiffness matrix of the unidirectional fibrous composites with the fibers oriented off-axis takes the form

$$\overline{C} = \begin{bmatrix} \overline{C}_{11} & \overline{C}_{12} & \overline{C}_{13} & 0 & 0 & \overline{C}_{16} \\ \overline{C}_{12} & \overline{C}_{22} & \overline{C}_{23} & 0 & 0 & \overline{C}_{26} \\ \overline{C}_{13} & \overline{C}_{23} & \overline{C}_{33} & 0 & 0 & \overline{C}_{36} \\ 0 & 0 & 0 & \overline{C}_{44} & \overline{C}_{45} & 0 \\ 0 & 0 & 0 & \overline{C}_{45} & \overline{C}_{55} & 0 \\ \overline{C}_{16} & \overline{C}_{26} & \overline{C}_{36} & 0 & 0 & \overline{C}_{66} \end{bmatrix} \tag{2}$$

Here, the components of $\overline{C}$ are given in Appendix C of Liang *et al.* (2006).

Following Zhao and Weng (1996, 1997) and Ju and Lee (2000), the probability distribution function of fiber debonding P_d at the level of hydrostatic tensile stress $(\overline{\sigma}_m)_1$ can be expressed as

$$P_d[(\overline{\sigma}_m)_1] = 1 - \exp\left[-\left(\frac{(\overline{\sigma}_m)_1}{S_0}\right)^M\right] \tag{3}$$

with $(\overline{\sigma}_m)_1 = (1 - \frac{2}{3}\nu_1)(\overline{\sigma}_{kk})_1$, where $(\overline{\sigma}_{kk})_1$ is the average hydrostatic tensile stress of the fibers, and the constants S_0 and M are the Weibull parameters.

According to Karihaloo and Fu (1989, 1990), the density of nucleated microcracks in concrete, denoted by ϕ_c, can be defined as

$$\phi_c = \begin{cases} \phi_{v0} & \varepsilon^a \le \varepsilon^{th} \\ \phi_{v0} + c_1\left(1 - \dfrac{\varepsilon^{th}}{\varepsilon^a}\right)^{c_2} & \varepsilon^a > \varepsilon^{th} \end{cases} \tag{4}$$

where ϕ_{v0} is the initial density of microcracks, ε^a is the current accumulated effective strain, $\varepsilon^{th} = \sqrt{\varepsilon_{ij}^{th}\varepsilon_{ij}^{th}}$ is the effective strain threshold below which no nucleation takes place, c_1 and c_2 are material constants. By incorporating Eqs. (3) and (4) into the constitutive equation Eq. (1), the progressive damage evolutions due to the interfacial fiber debonding in CFRP strips/sheets and nucleation of microcracks in concrete are taken into account in the constitutive relation. The details of the above constitutive model incorporating the damage mechanisms can be found in Liang *et al.* (2006).

The constitutive model based on Eq. (1) for the FRP sheets/strips is then implemented into the nonlinear FE program ABAQUS using the user-defined material subroutine (ABAQUS 2004) to model CFRP strips/sheets.

3. FE analysis of shear-deficient RC beams strengthened with CFRP U-wrap strips/sheets

3.1 Overview

Khalifa and Nanni (2002) examined the shear performance and modes of failure of rectangular simply supported RC beams designed with shear deficiencies. They fabricated twelve full-scale RC

beams with shear deficiencies. The variables investigated were presence of steel stirrups, shear span to effective depth (*a/d*) ratio, and amount and distribution of CFRP strips/sheets (Khalifa and Nanni 2002). Two main series designated SW and SO depending on the presence of steel stirrups in one of the half spans were tested. SW series consisted of four specimens and SO series consisted of eight specimens, and each series was divided into two subgroups according to the *a/d* ratio (Khalifa and Nanni 2002). The *a/d* ratio for SW3 and SO3 series is 3, while the *a/d* ratio for SW4 and SO4 series is 4.

In their experiments, one specimen from each series (SW3-1, SW4-1, SO3-1 and SO4-1) was left without strengthening as a control specimen, whereas eight beam specimens were strengthened with externally bonded CFRP strips/sheets with three different schemes. Three specimens (SO3-2, SO3-3, SO4-2) were strengthened with one-ply CFRP U-wrap strips; two specimens (SO3-4, SO4-3) with a one-ply continuous CFRP U-wrap sheet; and three specimens (SW3-2, SW4-2, SO3-5) with two-plies CFRP ($90^o/0^o$). All specimens were tested as simple span beams subjected to a four-point load, and load versus mid-span deflection (*p-u*) curves were plotted. Moreover, shear performance obtained from the experimental results was also compared with design shear performance obtained from modified ACI 318 (1995) for computing the shear capacity of RC beams strengthened with CFRP composite. The details of the experiment on RC beams strengthened with CFRP strips/sheets can be found in Khalifa and Nanni (2002).

Lee *et al.* (2007) investigated numerically the shear performance of the SO3 series, consisting of the Specimens SO3-1, SO3-2, SO3-4, and SO3-5, and the numerical results were compared with experimental results (Khalifa and Nanni 2002). This section focuses on the evaluation of shear performance of the SO4 and SW3 series models in Khalifa and Nanni (2002) to further investigate the shear strengthening performance of CFRP U-warp strips/sheets and to assess the predictive capability of the proposed FE analysis approach.

3.2 Performance prediction of SO4 series model

The configuration and reinforcement details for the SO4 series model are shown in Fig. 1 of Khalifa and Nanni (2002). Beams cast using stirrups within only half of the span as shown in the figure. The two different CFRP retrofit systems (Khalifa and Nanni 2002) shown in the figure are investigated: (a) Specimen SO4-2 strengthened with 90^o one-ply CFRP U-wrap strips, and (b) Specimen SO4-3 strengthened with a one-ply continuous CFRP U-wrap sheet having a 90^o fiber orientation.

Similar to the modeling conducted by Lee *et al*. (2007), the 3-D linear brick solid element C3D8 in the FE program ABAQUS is used to model concrete and CFRP strips/sheets, and the linear truss element T3D2 in the ABAQUS is used to model steel rebars and stirrups in concrete. The FE mesh used in this simulation is symmetric along the 3-axis and appropriate boundary condition on symmetric plane is applied as shown in Fig. 2(a). The loading and boundary conditions for specimen SO4-2 and SO4-3 are employed to simulate the four-point bending test as shown in Figs. 2(b) and (c), respectively. The Young's moduli of concrete, steel rebars and stirrups and CFRP strips/sheets are employed from Khalifa and Nanni (2002), and typical values of Poisson's ratio for concrete, steel rebars and stirrups and CFRP strips/sheets are used in the simulation. The material properties are listed in Table 1.

Control RC beam (SO4-1): The crack nucleation parameters ε^{th}, c_1, and c_2 of concrete (Liang *et al.* 2006) are estimated using the trial-and-error method in accordance with the experimentally

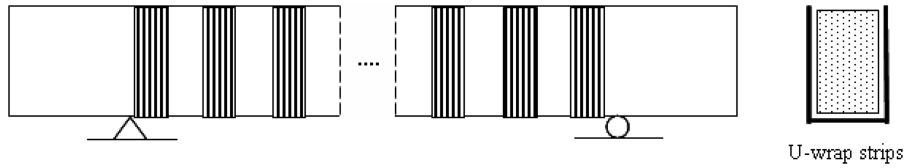

(a) One-ply CFRP U-wrap strips (specimen SO4-2)

(b) One-ply continuous CFRP U-wrap sheet (specimen SO4-3)

Fig. 1 Schematics of the two CFRP retrofit systems: (a) One-ply CFRP (U-wrap) strips (specimen SO4-2); (b) One-ply continuous CFRP (U-wrap) sheet (specimen SO4-3) (reproduced from Khalifa and Nanni 2002)

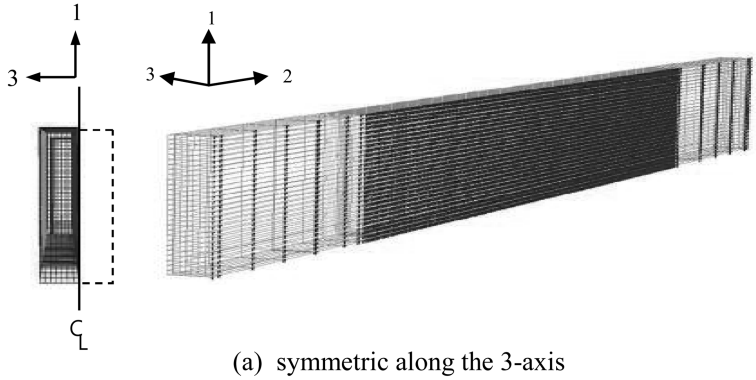

(a) symmetric along the 3-axis

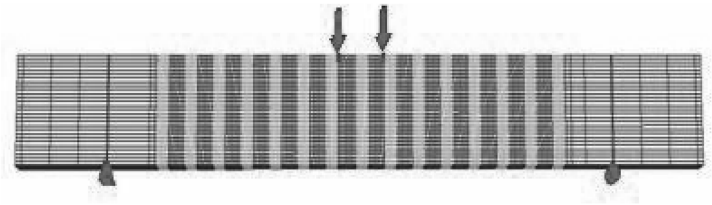

(b) 50mm CFRP strips (SO4-2 specimen)

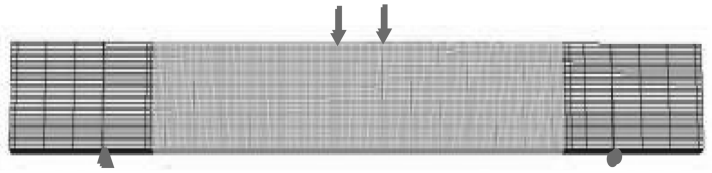

(c) A continuous CFRP U-wrap sheet (SO4-3 specimen)

Fig. 2 The FE mesh is symmetric along the 3-axis (a) and loading/boundary condition for four point bending test : the Specimens SO4-2 (b) and SO4-3 (c)

Table 1 Material properties used in the simulation

	Concrete	CFRP strips/sheets (fiber only)	Steel rebars and stirrups
Young's modulus (GPa)	25.0	228.0	200.0
Poisson's ratio	0.17	0.20	0.30

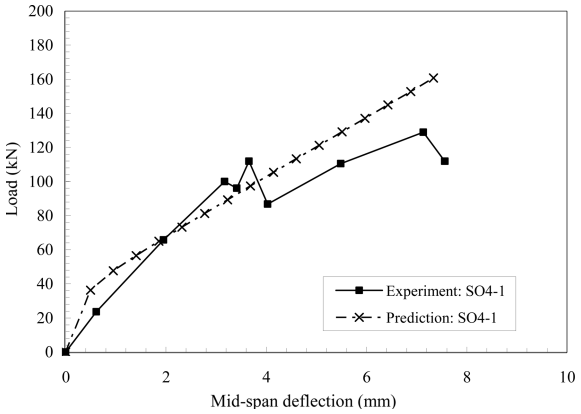

Fig. 3 The present predicted *p-u* curve of the control beam (SO4-1) that best fits to the experimental data produced by Khalifa and Nanni (2002)

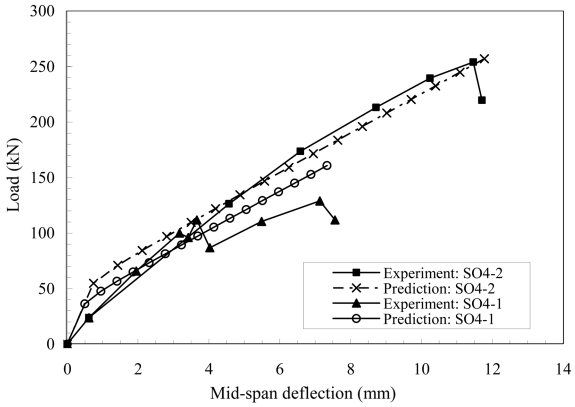

Fig. 4 The comparison of *p-u* curves between the present prediction and the experimental data reported by Khalifa and Nanni (2002) on the RC beam strengthened with one-ply CFRP U-wrap strips (SO4-2)

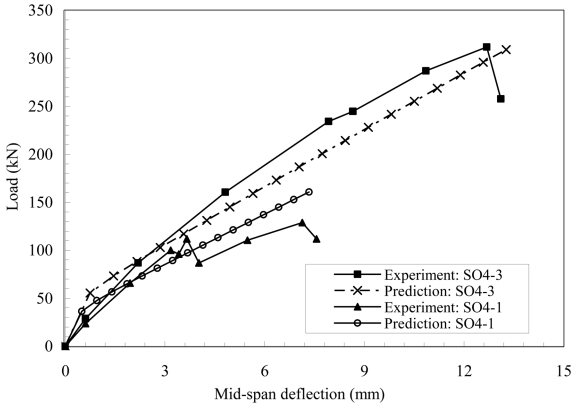

Fig. 5 The comparison of *p-u* curves between the present prediction and the experiment conducted by Khalifa and Nanni (2002) on the RC beam strengthened with a one-ply continuous CFRP U-wrap sheet (SO4-3)

obtained *p-u* curve (Khalifa and Nanni 2002) on an un-strengthened RC beam (control beam). Fig. 3 shows the predicted *p-u* curve of the control beam that best fits to the experiment. The estimated crack nucleation parameters of concrete are $\varepsilon^{th} = 0.5 \times 10^{-6}$, $c_1 = 0.925$, $c_2 = 10.8$.

Strengthened RC beams with CFRP strips/sheets (SO4-2, SO4-3): The fiber debonding parameters of CFRP strips/sheets (Liang *et al.* 2006) involving the present simulation are assumed to be: $S_0 = 22.5 \times 10^2$ MPa, $M = 4.0$. The predicted *p-u* curves of the RC specimens strengthened with one-ply

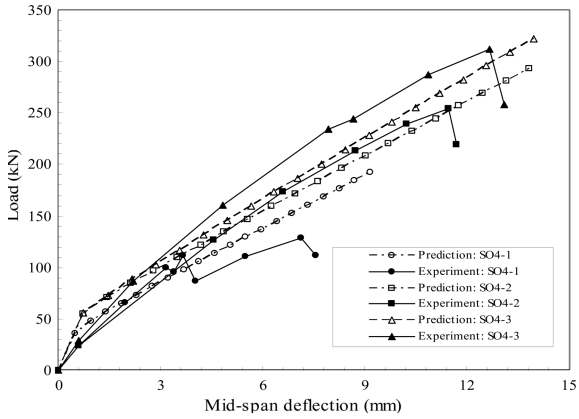

Fig. 6 The *p-u* curves of the Specimens SO4-1, SO4-2 and SO4-3

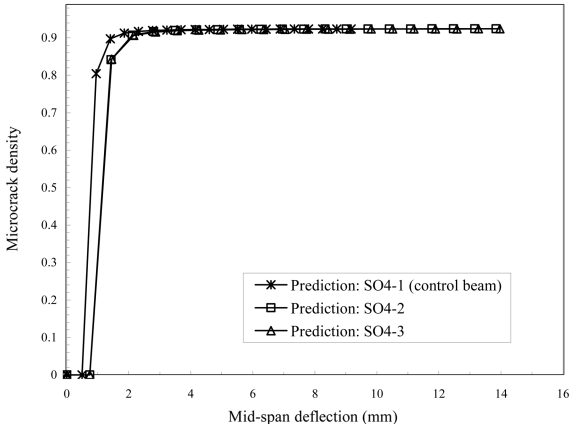

Fig. 7 The evolution of the microcrack density in concrete versus deflection corresponding to Figs. 3-5

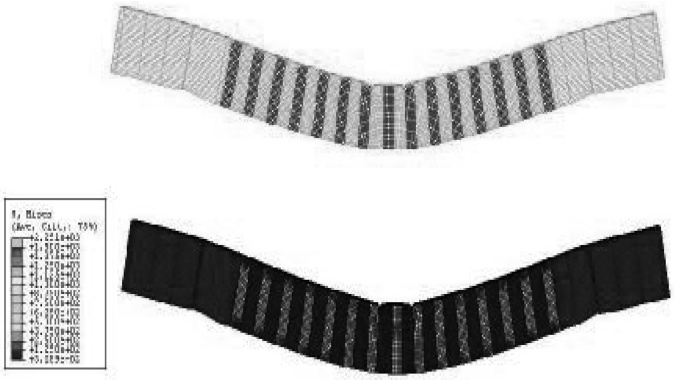

(a) Specimen SO4-2

(b) Specimen SO4-3

Fig. 8 The deformed shape and von-Mises effective stress of the Specimens SO4-2 and SO4-3 during the four-point bending tests

CFRP strips and a one-ply continuous CFRP sheet (on the basis of the material properties in Table 1, the estimated crack nucleation parameters of concrete and the assumed fiber debonding parameters) are shown in Figs. 4 and 5, respectively. The predicted *p-u* curves match the experimental results (Khalifa and Nanni 2002) well as shown in these figures. It should be noted that the predicted *p-u* curves are shown to the deflection at which the experimentally obtained *p-u* curves were terminated in these figures. The comparison is also made for the predicted *p-u* curves of the Specimens SO4-1, SO4-2 and SO4-3 in Fig. 6. The experimentally obtained *p-u* curves of the SO4-1, SO4-2 and SO4-3 (Khalifa and Nanni 2002) are also plotted in the figure for comparison. It is observed that the RC beam strengthened with a one-ply continuous CFRP U-wrap sheet (Specimen SO4-3) is capable of sustaining larger loads and absorbing more energy at equal deflections in comparison with the RC beam strengthened with one-ply CFRP U-wrap strips (Specimen SO4-2). The predicted microcrack density in concrete corresponding to Fig. 6 is plotted against the mid-span deflection for the control beam (Specimen SO4-1) and the strengthened beams (Specimens SO4-2 and SO4-3) in Fig. 7. The predicted deformed shape and von-Mises effective stress of the RC beams during the four-point bending tests are shown in Fig. 8.

3.3 Performance prediction of SW3 series model

Khalifa and Nanni (2002) investigated experimentally the shear performance of retrofitted RC beams having different stirrup lay-ups (SO3 and SW3 series models). SW3 series model was reinforced with steel stirrups on the entire span as illustrated in Fig. 1 of Khalifa and Nanni (2002), whereas stirrups were provided within only a half span of the SO3 series model. Details of the stirrups lay-ups can be found in Khalifa and Nanni (2002).

A series of numerical four-point bending tests on the SW3 series are performed to investigate the effect of different stirrup lay-ups on the shear performance of CFRP strengthened RC beams. The crack nucleation parameters used in the simulation for the SW3 series model are estimated in accordance with the unstrengthened (control) beam (SW3-1) as follows: $\varepsilon^{th} = 0.15 \times 10^{-5}$, $c_1 = 0.925$, $c_2 = 10.8$. In addition, we employ the same fiber debonding parameters as those used in the previous simulations.

The present predicted and experimental *p-u* curves for the SW3 series, consisting of the control

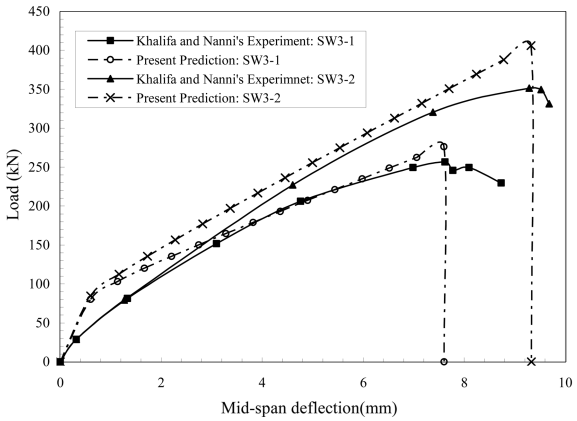

Fig. 9 The comparison of *p-u* curves between the present prediction and the experiment conducted by Khalifa and Nanni (2002) on the SW3 series model

beam (SW3-1) and CFRP strengthened beam (SW3-2), are plotted in Fig. 9. The predicted (Lee *et al.* 2007) and experimental (Khalifa and Nanni 2002) *p-u* curves for the Specimens SO3-1 and SO3-5 can be found in Figs. 3 and 6 of Lee *et al.* (2007). The energy absorbed in specimens during deformation is obtained by calculating the area under the *p-u* curve using the Origin software (from www.originlab.com).

In Figs. 3 and 6 of Lee *et al.* (2007) and Fig. 9, the areas under the predicted *p-u* curves up to the deflection corresponding to the experimentally obtained peak load are computed to assess the energy absorbing capacity of the CFRP strips/sheets applied on RC beams with different stirrup lay-ups. 205% and 69% increases in energy absorption over the control specimens are observed with the Specimens SO3-5 and SW3-2, respectively. It can be concluded from the above results that the shear strengthening performance of CFRP U-wrap strips/sheets is more pronounced when they are applied on RC beams without stirrups in a portion of shear span. The findings of this numerical simulation correspond with Khalifa and Nanni (2002)'s experimental observations.

3.4 Parametric analysis on microcrack nucleation parameters

Microcrack nucleation parameters ε^{th}, c_1, and c_2 (Liang *et al.* 2006, Lee and Liang 2004) are related to the nucleation of microcracks in concrete. To illustrate the influence of the parameters ε^{th}, c_1, and c_2 on the microcrack density evolution in concrete and to evaluate the constitutive model sensitivity to the microcrack nucleation parameters, a parametric analysis is conducted. For comparison, numerical four-point bending tests on the control beam (SO4-1) are conducted on the basis of the material properties and fiber debonding parameters used in the previous simulations.

Four different values of ε^{th} are used in the present simulation: $\varepsilon^{th} = 0.5 \times 10^{-8}$, 0.5×10^{-7}, 0.5×10^{-6}, 0.5×10^{-5}. The predicted *p-u* curves of RC beams with these values of ε^{th} are shown in Fig. 10. Fig. 11 shows the predicted evolution of the numbers of microcracks per unit volume versus deflection corresponding to Fig. 10. It is observed from Figs. 10 and 11 that as the value of ε^{th} continues to decrease, the beam exhibits a lower *p-u* response due to the rapid nucleation of microcracks.

Fig. 12 shows the predicted *p-u* curves of RC beams with various values of c_1: $c_1 = 0.925 \times 10^{-2}$,

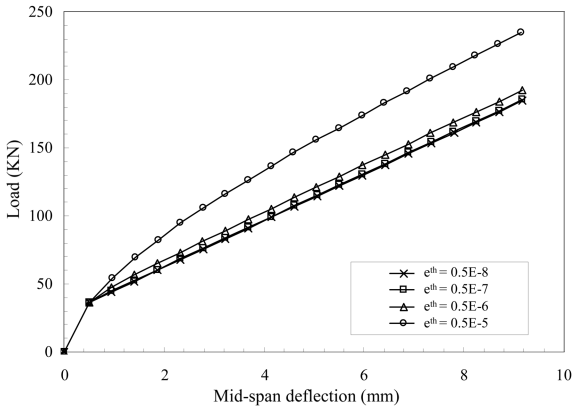

Fig. 10 The predicted *p-u* curves of RC beams with various values of ε^{th}

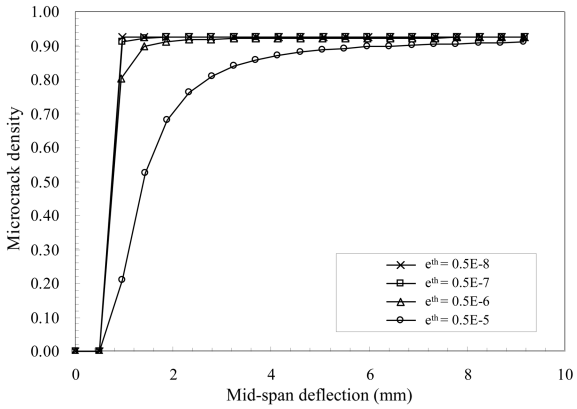

Fig. 11 The predicted evolution of numbers of microcracks in unit volume in RC beams with various values of ε^{th}

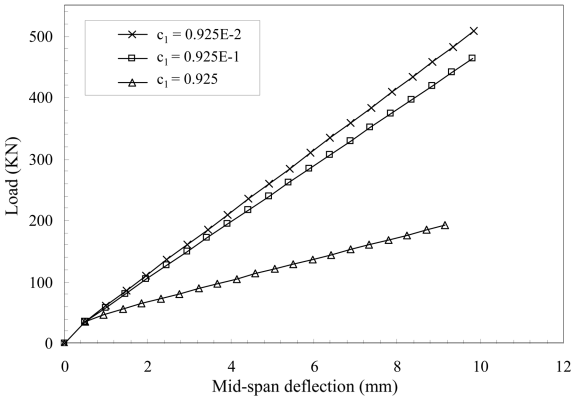

Fig. 12 The predicted *p-u* curves of RC beams with various values of c_1

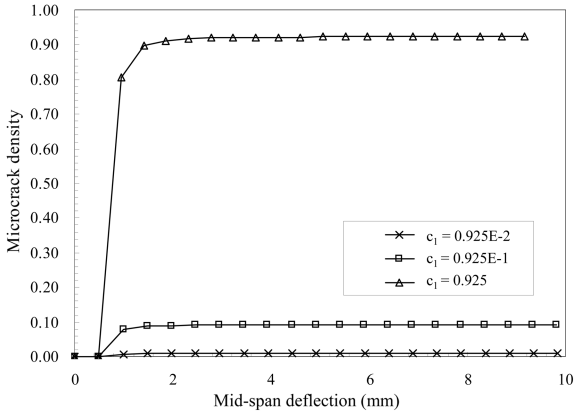

Fig. 13 The predicted evolution of the numbers of microcracks in unit volume in RC beams with various values of c_1

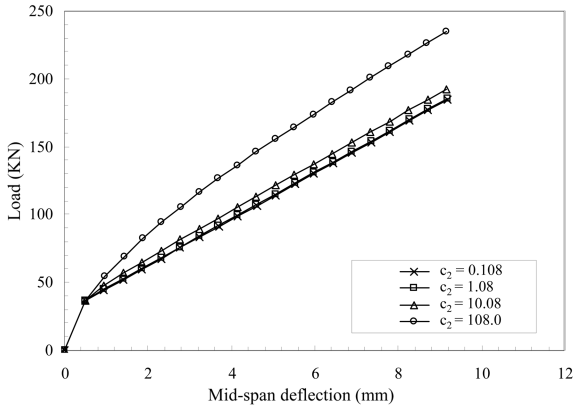

Fig. 14 The predicted *p-u* curves of RC beams with various values of c_2

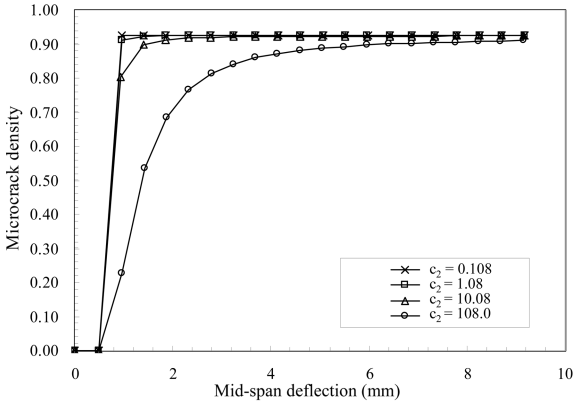

Fig. 15 The predicted evolution of the numbers of microcracks in unit volume in RC beams with various values of c_2

0.925×10^{-1}, 0.925. The predicted evolution of the numbers of microcracks in unit volume corresponding to Fig. 12 is shown in Fig. 13. It is observed from Fig. 13 that the microcrack density in concrete continues to increase as the value of c_1 increases. A parametric analysis for c_2 is also conducted and the results are plotted in Figs. 14 and 15. Fig. 14 illustrates the numerical results for various values of c_2: c_2 = 0.108, 1.08, 10.8, 108.0, and the predicted evolution of the numbers of microcracks in unit volume corresponding to Fig. 14 is shown in Fig. 15. It is found from Figs. 14 and 15 that the lower value of c_2 causes an increase in microcrack density at early stages of loading, resulting in a lower *p-u* response. However, more systematic parametric analysis on the microcrack nucleation parameters are needed to further evaluate the sensitivity of the parameters and to provide (upper-and lower-) limits of each parameter.

4. FE analysis of shear-deficient RC beams strengthened with non U-wrap type CFRP strips/sheets

In this section, a series of numerical four-point bending tests are carried out using the FE program ABAQUS for investigating the shear and flexural strengthening performance of non U-wrap type CFRP strips/sheets on the basis of the material properties and fiber debonding and microcrack nucleation parameters used in the SO4 series model simulations. *The shear strengthening performance* of one-ply CFRP strips having the 50 mm width and a one-ply continuous CFRP sheet is evaluated by modeling the CFRP strips and the CFRP sheet on both vertical sides of the shear-deficient RC beam (Specimen SO4 series model), whereas *the flexural strengthening performance* of the CFRP strips and the CFRP sheet is computed by modeling them on the bottom of the shear-

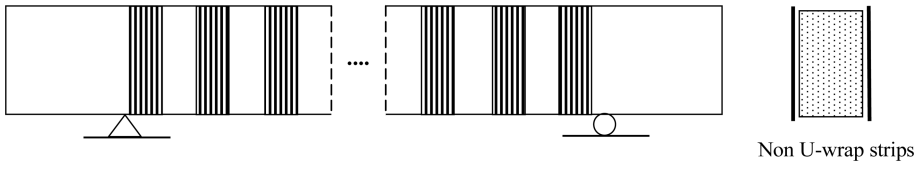

(a-1)

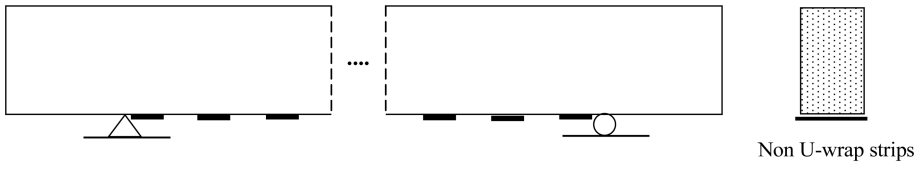

(a-2)

(a) CFRP strips on vertical faces (a-1) and bottom face (a-2)

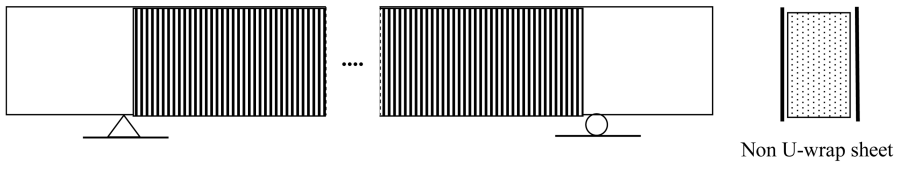

(b-1)

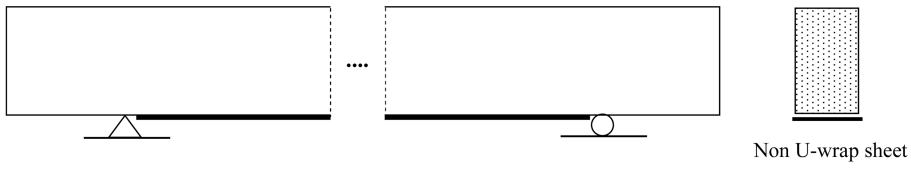

(b-2)

(b) CFRP sheet on vertical faces (b-1) and bottom face (b-2)

Fig. 16 Schematics of the various CFRP strengthening systems used in the simulation: (a) CFRP strips; (b) CFRP sheet

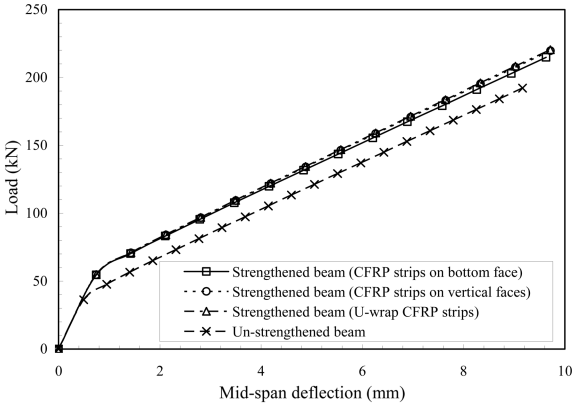

Fig. 17 The comparison of predicted *p-u* curves of RC beams strengthened with the non U-wrap type CFRP strips on vertical faces, the non U-wrap type CFRP strips on bottom face and the U-wrap type CFRP strips

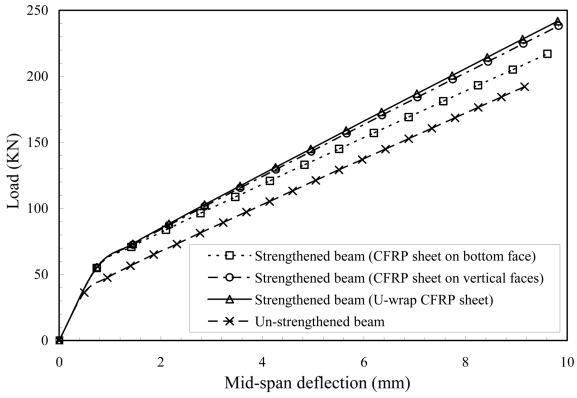

Fig. 18 The comparison of predicted *p-u* curves of RC beams strengthened with the non U-wrap type CFRP sheet on vertical, the non U-wrap type CFRP sheet on bottom face and the U-wrap type CFRP sheet

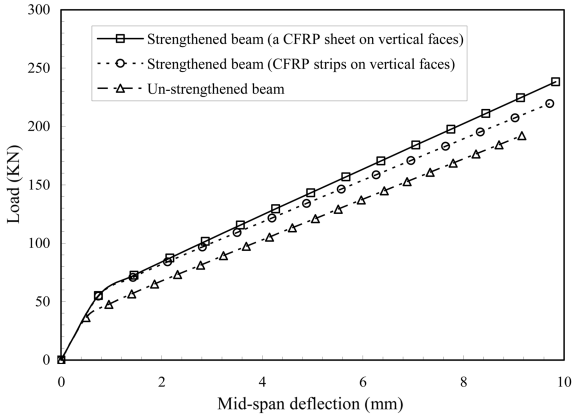

Fig. 19 The comparison of predicted *p-u* curves between beams strengthened with CFRP strips and a CFRP sheet on vertical faces

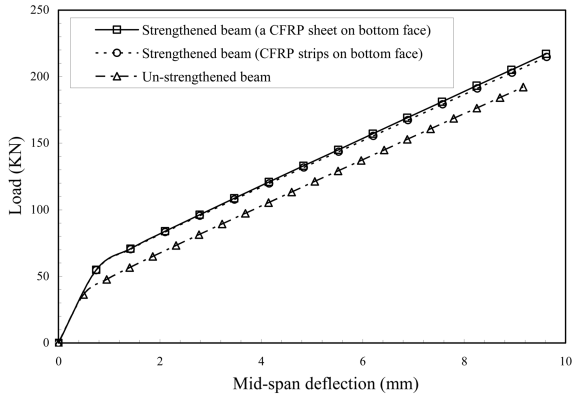

Fig. 20 The comparison of predicted *p-u* curves between beams strengthened with CFRP strips and a CFRP sheet on bottom face

deficient RC beam as shown in Fig. 16.

Fig. 17 illustrates the flexural and shear strengthening performance of the CFRP strips, while Fig. 18 shows the flexural and shear strengthening performance of the CFRP sheet. The numerical results indicate that the improvement in load-carrying capacity by the use of side CFRP strips is nearly the same as that by the use of bottom CFRP strips, whereas the *p-u* curve is slightly higher with the use of side CFRP sheets in comparison with the use of bottom CFRP sheets.

The predicted *p-u* curves of the shear-deficient RC beams strengthened with the CFRP strips and the CFRP sheet on both vertical sides are compared in Fig. 19. The increase in shear performance of the RC beams is shown to be more pronounced with the use of CFRP sheet on both vertical sides. Fig. 20 shows the comparison of the predicted *p-u* curves of the shear-deficient RC beams strengthened with the CFRP strips and the CFRP sheet on the bottom. The CFRP strips and the

CFRP sheet exhibit nearly the same load-carrying capacity.

Simultaneous use of bottom and side CFRP strips and sheet on shear-deficient RC beams is also compared with the above mentioned non U-wrap type CFRP strips/sheets. Figs. 17 and 18 show the comparison of the predicted *p-u* curves of the shear-deficient RC beams strengthened with the U-wrap and the non U-wrap type CFRP strips and sheets, respectively. It is observed from these figures that the load-carrying capacity of both the beam strengthened with the non U-wrap type CFRP strips on the vertical faces and the beam strengthened with the U-wrap type CFRP strips is shown to be slightly higher than that of the beam strengthened with the non U-wrap type CFRP strips on the bottom face, whereas both the beam strengthened with the U-wrap type CFRP sheet and the beam strengthened with the non U-wrap type CFRP sheet on the vertical faces have a moderately higher load-carrying capacity than the beam strengthened with the non U-wrap type CFRP sheet on the bottom face.

5. Conclusions

An FE analysis approach to evaluate the performance of RC beams strengthened with CFRP strips/sheets has been presented. Based on a micromechanics-based constitutive model for laminated composites (Liang *et al.* 2006) implemented into the finite element program ABAQUS, a series of numerical four-point bending tests are conducted to investigate the shear performance of RC beams strengthened with CFRP strips/sheets and to quantify shear strengthening performance of the CFRP repair systems.

The present predictions are compared with experimental data (Khalifa and Nanni 2002) to assess the accuracy of the proposed FE analysis approach. A series of numerical tests are conducted to investigate the influence of stirrup lay-ups on the shear strengthening performance of the CFRP strips/sheets, to illustrate the influence of the damage parameters on the microcrack density evolution in concrete, and to investigate the shear and flexural strengthening performance of CFRP strips/sheets. The findings from this numerical study can be summarized as follows:

1. The predicted *p-u* curves of un-strengthened and strengthened RC beams match the experimental results (Khalifa and Nanni 2002) well.
2. The RC beam strengthened with a one-ply continuous CFRP U-wrap sheet is capable of sustaining larger loads and absorbing more energy at equal deflections in comparison with the RC beam strengthened with one-ply CFRP U-wrap strips.
3. From the parametric analysis, crack nucleation parameters ε^{th}, c_1, and c_2 are shown to affect the shear performance of CFRP strengthened RC beams. As the values of ε^{th} and c_2 decrease and the value of c_1 increases, the RC beam exhibits a lower *p-u* response due to mainly the rapid nucleation of microcracks.
4. The shear strengthening performance of the CFRP U-wrap strips/sheet is more pronounced when the CFRP retrofit systems are applied on RC beams having the absence of stirrups in a portion of shear span.
5. Both the beam strengthened with the non U-wrap type CFRP strips on the vertical faces and the beam strengthened with the U-wrap type CFRP strips have a slightly higher load-carrying capacity than the beam strengthened with the non U-wrap type CFRP strips on the bottom face, whereas both the beam strengthened with the U-wrap type CFRP sheet and the beam strengthened with the non U-wrap type CFRP sheet on the vertical faces have a moderately

higher load-carrying capacity than the beam strengthened with the non U-wrap type CFRP sheet on the bottom face.

The present numerical study has shown that the proposed FE analysis approach is suitable for the performance prediction of RC beams strengthened with CFRP strips/sheets. However, damage parameters in the constitutive model need to be experimentally characterized for more accurate and realistic performance prediction of retrofitted or strengthened RC structures with CFRP strips/sheets. It should also be noted that the proposed FE analysis approach cannot account for the failure of CFRP wrapped RC beams since the model does not incorporate any failure criteria for concrete and CFRP strips/sheets. This issue is beyond the scope of the present work; nevertheless, it could be a subject of future research.

Acknowledgements

This research was sponsored by the Ministry of Science and Technology, Korea, for the financial support by a grant (R11-2002-101-02003, 2008) from the Smart Infra-Structure Technology Center (SISTeC).

References

ABAQUS Example Problems Manual, Version 6.5, Hibbitt, Karlsson & Sorensen, Inc., Pawtucket, RI, 2004.

ACI Committee 318 : Building code requirements for structural concrete (ACI 348-5) and commentary (ACI 318R-95), pp.369, 1995.

Arduini, M., Tommaso, A.D. and Nanni, A. (1997), "Brittle failure in FRP plate and sheet bonded beams", *ACI Struct. J.*, **94**, 363-371.

Chajes, M.J., Thomson, T.A., Januszka, T.F. and Fin, W. (1994), "Flexural strengthening of concrete beams using externally bonded composite materials", *Constr. Building Mater.*, **8**, 191-201.

Cheng, Z.Q. and Batra, R.C. (1999), "Exact eshelby tensor for a dynamic circular cylindrical inclusion", *J. Appl. Mech.*, **66**, 563-565.

Ghosh, K. and Karbhari, V.M. (2007), "Evaluation of strengthening trough laboratory testing of FRP rehabilitated bridge decks after in-service loading", *Comp. Struct.*, **77**, 206-222.

Herakovich, C.T. (1998), *Mechanics of Fibrous Composites*, John Wiley and Sons, New York.

Jayaprakash, J., Sarnad, A.A.A. and Abbasovictf, A.A. (2007), "Repair of precracked RC rectangular shear beams using CFRP strip technique", *Struct. Eng. Mech.*, **26**, 427-439.

Jones, J.X., Heymsfield, E. and Durham, S.A. (2004), "Fiber-reinforced polymer shear strengthening of short-span, precast channel beams in bridge superstructures", Transportation Research Record: Journal of Transportation Research Board, No. 1892, 56-65.

Jones, R., Swamy, R.N., Bloxham, J. and Bouderbalah, A. (1980), "Composite behavior of concrete beams with epoxy bonded external reinforcement", *Int. J. Cement Comp.*, **2**, 91-107.

Ju, J.W. and Chen, T.M. (1994a), "Micromechanics and effective moduli of elastic composites containing randomly dispersed ellipsoidal inhomogeneities", *Acta Mech.*, **103**, 103-121.

Ju, J.W. and Chen, T.M. (1994b), "Effective elastic moduli of two-phase composites containing randomly dispersed spherical inhomogeneities", *Acta Mech.*, **103**, 123-144.

Ju, J.W. and Lee, H.K. (2000), "A micromechanical damage model for effective ealstoplastic behavior of ductile matrix composites considering evolutionary complete particle debonding", *Comput. Meth. Appl. M.*, **183**, 201-222.

Karihaloo, B.L. and Fu, D. (1989), "A damage-based constitutive law for plain concrete in tension", *Euro. J.*

Mech., A-Solids, **8**, 373-384.
Karihaloo, B.L. and Fu, D. (1990), "Orthotropic damage model for plain concrete in tension", *ACI Mater. J.*, **87**, 62-67.
Khalifa, A. and Nanni, A. (2002), "Rehabilitation of rectangular simply supported RC beams with shear deficiencies using CFRP composites", *Constr. Building Mater.*, **16**, 135-146.
Khalifa, A., De Lorenzis, L. and Nanni, A. (2000), "FRP composites for shear strengthening of RC beams", *Proc. 3rd Inter. Conf. on Advanced Composite Materials in Bridges and Structures*, Ottawa, Canada, 137-144, August 15-18.
Lee, H.K. and Liang, Z. (2004), "Computational modeling of the response and damage behavior of fiber-reinforced cellular concrete", *Comput. Struct.*, **82**(7-8), 581-592.
Lee, H.K., Kim, B.R. and Ha, S.K. (2007), "Numerical evaluation of shear strengthening performance of FRP sheets/strips and sprayed epoxy coating repair systems", Composites Part B: Engineering, under review.
Leung, H.Y. (2002), "Strengthening of RC beams: Some experimental findings", *Struct. Survey*, **20**, 173-181.
Liang, Z., Lee, H.K. and Suaris, W. (2006), "Micromechanics-based constitutive modeling for unidirectional laminated composites", *Int. J. Solids Struct.*, **43**, 5674-5689.
Niu, H., Vasquez, A. and Karbhari, V.M. (2006), "Effect of materials configuration on strengthening of concrete slabs by CFRP composites", *Comp. Part B.*, **37**, 213-226.
Norris, T., Saadatmanesh, H. and Mohammad, R.E. (1997), "Shear and flexural strengthening of R/C beams with carbon fiber sheets", *J. Struct. Eng.*, ASCE, **123**, 903-911.
Oehlers, D.J., Nguyen, N.T. and Bradford, M.A. (2000), "Retrofitting by adhesive bonding steel plates to the sides of RC beams. Part 2: Debonding of plates due to shear and design rules", *Struct. Eng. Mech.*, **9**, 505-518.
Origin software, downloded from www.originlab.com
Saadatmanesh, H. and Ehsani, M.R. (1991), "RC beams strengthened with GFRP plates: An experimental study", *J. Struct. Eng.*, **117**, 3417-3433.
Wenwei, W. and Guo, L. (2006), "Experimental study and analysis of RC beams strengthened with CFRP laminates under sustaining load", *Int. J. Solids Struct.*, **43**, 1372-1387.
Zhao, Y.H. and Weng, G.J. (1996), "Plasticity of a two-phase composite with partially debonded inclusion", *Int. J. Plasticity*, **12**, 781-804.
Zhao, Y.H. and Weng, G.J. (1997), "Transversely isotropic moduli of two partially debonded composites", *Int. J. Solids Struct.*, **34**, 493-507.